Working Paper Series

Quarantine, Contact Tracing, and Testing: Implications of an Augmented SEIR Model

WP 21-08

Andreas Hornstein
Federal Reserve Bank of Richmond

**FEDERAL RESERVE BANK
OF RICHMOND**®

Richmond • Baltimore • Charlotte

Quarantine, Contact Tracing, and Testing:
Implications of an Augmented SEIR Model *

Andreas Hornstein

Federal Reserve Bank of Richmond

andreas.hornstein@rich.frb.org

First Version March 25, 2020
This Version May 11, 2021

Abstract

I incorporate quarantine, contact tracing, and random testing in the basic SEIR model of infectious disease diffusion. A version of the model that is calibrated to known characteristics of the spread of COVID-19 is used to estimate the transmission rate of COVID-19 in the United States in 2020. The transmission rate is then decomposed into a part that reflects observable changes in employment and social contacts and a residual component that reflects disease properties and all other factors that affect the spread of the disease. I then construct counterfactuals for an alternative employment path that avoids the sharp employment decline in the second quarter of 2020 but also results in higher cumulative deaths due to a higher contact rate. For the simulations, a modest permanent increase of quarantine effectiveness counteracts the increase in deaths, and the introduction of contact tracing and random testing further reduces deaths, although at a diminishing rate. Using a conservative assumption on the statistical value of life, the value of improved health outcomes from the alternative policies far outweighs the economic gains in terms of increased output and the potential fiscal costs of these policies.

1 Introduction

From March to April 2020, after a number of states introduced stay-at-home orders in response to the emerging COVID-19 pandemic, employment in the United States declined precipitously, by about 15 percent. Upon relaxing the stay-at-home orders, employment recovered to within 6 percent of pre-pandemic levels in the late summer of 2020. The decline in work-related contacts and social contacts associated with these stay-at-home orders arguably helped contain the pandemic and the number of disease-related deaths but came at the cost of lost output. In this paper, I argue that a more targeted approach, such as improved quarantine, contact tracing, and random testing, could have attained similar or better disease-related outcomes for an alternative employment path that avoided the sharp and deep decline. Furthermore, the benefits of this alternative approach, in terms of the value of lives saved, far outweigh its potential costs.

Indiscriminate social distancing limits the spread of COVID-19 because it reduces contact rates for all individuals, whether they are infectious or not. Quarantine is less disruptive in that it only removes known infectious individuals. Clearly, infectious individuals who display symptoms can be quarantined, but a feature of COVID-19 is that even individuals who do not display symptoms can be infectious. Contact tracing can work backwards from newly identified symptomatic individuals to identify individuals who may have been infected but do not yet display any symptoms. Random testing of the population is another way to identify individuals who are infectious but asymptomatic.

I study the effects of quarantine, contact tracing, and random testing in a modified susceptible-exposed-infected-recovered (SEIR) model where I differentiate between asymptomatic and symptomatic infected individuals. The modified SEIR model is calibrated to the known characteristics of COVID-19 and is then used to infer the transmission rate of COVID-19 from data on daily deaths. Information on employment and social mobility indices is then used to separate out the impact of work contacts on the transmission rate. This procedure suggests that the shift toward work at home—as documented in Bick, Blandin and Mertens (2021)—had a larger impact on overall work contacts than the reduced employment in April and May 2020. I then assume an alternative employment path that avoids the sharp decline and rebound of employment, thus avoiding the output losses associated with the employment reductions.

The alternative employment path implies a higher overall transmission rate and more fatalities. We consider various combinations of improved quarantine measures, contact tracing, and random testing to counteract the increased contact rate from the alternative employment path. The simulations suggest that a moderate and permanent increase of the quarantine

rate much better contains cumulative deaths over the second half of the year, even though it is initially not as effective as the steep but temporary actual employment reductions in the first part of the year. In particular, in the simulations, a moderate permanent increase of the quarantine rate prevents the surge of infections and deaths at the end of the year. Adding contact tracing and random testing yields additional reductions of cumulative deaths but not of the same magnitude as the initial increase of quarantine effectiveness.

We provide some rough estimates of the gains from avoided output losses and deaths and the potential fiscal costs of the simulated alternative policies. For a conservative estimate of the statistical value of a life ($7 million), the gains from improved health outcomes, in the range of $3.5 trillion to 5 trillion, far outweigh gains from avoided output loss, about $500 billion, and the potential fiscal costs of the program, between $60 billion and $150 billion.

One can have well-founded reservations on the use of the kind of model described here for policy analysis, and Jewell, Lewnard and Jewell (2020) provide an extensive list of these reservations. On the other hand, short of running actual "experiments" on an economy, models like the one described here provide some guidance on possible outcomes for these policy interventions.

1.1 Related work in epidemiology

We work with an augmented version of the standard SEIR model of disease diffusion with Poisson arrival rates for health-state changes and implied exponential distributions for stage duration. Most epidemiological work on quarantine and contact tracing models these interventions as setting aside a fraction of newly infected individuals and gradually moving them to a quarantine state, similar to the transition between health states. The effectiveness of these interventions is then determined by the share and speed parameters, see for example Wearing, Rohani and Keeling (2005) or Feng (2007). Lipsitch et al. (2003) use a similar approach to study the issue of contact tracing in the context of the SARS epidemic.

Compared with this epidemiological work, the approach I take is more direct: some infected individuals can be identified, and they are immediately quarantined, but only a fraction of quarantined individuals can be excluded from the infectious pool. This "targeted quarantine" model makes the interpretation of its effectiveness more transparent.

1.2 Related work by economists using SIR-type models

There has been an outburst of work in economics on COVID-19, much of it appearing in the CEPR online publication *Covid Economics, Vetted and Real-Time Papers.*[1]

---

[1]https://cepr.org/content/covid-economics-vetted-and-real-time-papers-0#block-block-9.

Baqaee, Farhi, Mina and Stock (2020) are closest in spirit to this paper in that they study the implications of alternative paths for employment and non-pharmaceutical interventions, including quarantine, for output losses and fatalities. Their environment contains more demographic and economic detail; they differentiate by age groups and industries, but their approach to quarantine follows the standard epidemiological literature, and they interpret contact tracing and testing as changes in the rate at which infectious individuals are quarantined. Baqaee et al. (2020) also find non-pharmaceutical interventions to be preferable to employment reductions.

Berger, Herkenhoff, Huang and Mongey (2021) and Piguillem and Shi (2020) study random testing in a SEIR-type model of targeted quarantine. Berger et al. (2021) study the relative effectiveness of tests and argue that the frequent use of cheap low-sensitivity tests dominates the infrequent use of expensive perfect tests. Neither of these papers considers contact tracing.

My approach to infer the diffusion of COVID-19 from data on daily deaths is based on Fernandez-Villaverde and Jones (2020) and Atkeson, Kopecky and Zha (2020). In a simple SEIR model, there is a linear progression from being susceptible to possible death. Given this structure, one can work backwards and infer current infected individuals from future deaths in a parameterized version of the model. My approach to extract the effect of employment changes on the transmission rate is related to Baqaee et al. (2020). My approach to estimate the potential cost and benefits of alternative policies uses the value of a statistical life (VSL) and is related to Greenstone and Nigam (2020) and Cutler and Summers (2020). Greenstone and Nigam (2020) use the VSL to calculate the benefits from reduced mortality rates for various pandemic scenarios in the large-scale pandemic model of Ferguson et al. (2020). Cutler and Summers (2020) estimate the costs of COVID-19 from reduced output, increased mortality, and negative health outcomes for survivors.

Finally, this paper is a substantially revised version of Hornstein (2020), which considered a more stylized version of social distancing as a constant but temporary reduction in contact rates in the face of a constant transmission rate. In terms of health outcomes, this paper focuses on fatalities, whereas the pandemic model in Hornstein (2020) was intended as a stylized version of Ferguson et al. (2020) and also considered the implications for hospital stays and the use of intensive care units.

Figure 1: The SIR Model
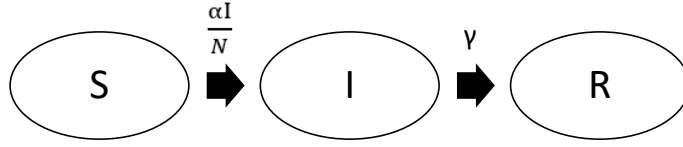
2 The basic SIR model

Define the stock of susceptible population S, infected and infectious population I, and recovered population R. Total population is

$$N = S + I + R. \tag{1}$$

Individuals transition sequentially between the states determined by Poisson processes with given arrival rates. Assume that the disease transmission rate for a given encounter is α, that the recovery rate from the disease is γ, and that recovered individuals are immune to the disease. See Figure 1 for a graphic representation.

Total disease transmission, M, following from meetings between the susceptible and infected population is then,

$$M = \left(\alpha \frac{S}{N} \right) I, \tag{2}$$

where the term in brackets is the new infections caused per infected individual. The dynamics are described by the differential equations

$$\dot{S} = -\alpha \frac{IS}{N}, \tag{3}$$

$$\dot{I} = \alpha \frac{IS}{N} - \gamma I, \tag{4}$$

$$\dot{R} = \gamma I. \tag{5}$$

The infectious group grows at the rate

$$\hat{I} = \left(\frac{\alpha}{\gamma} \frac{S}{N} - 1 \right) \gamma.$$

Assume that the initial value for the population share of susceptible individuals is essentially one, $S(0) \approx N$. Then, the number of infected people is initially increasing if

$$\mathcal{R}_0 = \frac{\alpha}{\gamma} > 1. \tag{6}$$

The ratio $\mathcal{R}_0$ is called the basic reproduction number because at time zero it is approximately the average number of new infections caused by an infected individual before that individual recovers,

$$\int_0^\infty \left[\alpha \frac{S(\tau)}{N} \tau \right] \gamma e^{-\gamma\tau} d\tau \approx \frac{\alpha}{\gamma} = \mathcal{R}_0,$$

where the first term in the integral is the average number of infections over a time interval τ, and the second term is the probability of staying infectious for that time.

# 3   An extended SEIR model

I now extend the basic SIR model to explore the relative merits of various policy measures, such as social distancing, quarantine, contact tracing, and random testing in a unified framework. Susceptible individuals are exposed to the infection but are not immediately infectious. Exposed individuals become infectious, but they initially do not show any symptoms. After some time, asymptomatic infected individuals do show symptoms of the disease and can be quarantined. Symptomatic infected individuals either recover over time and become immune, or they die.

Introducing the exposed state into the SIR model is standard, and we do it because there is evidence for a non-negligible latency period for the case of COVID-19. Adding an exposed state changes the dynamics of the model, e.g., it tends to change peak infection rates, but it usually does not affect terminal outcomes much. Getting the disease dynamics right is important, since in the next section we will account for the spread of the disease through the lens of the model.

We make a distinction between asymptomatic and symptomatic infectious individuals because we want to study the role of quarantine and contact tracing as alternative policy tools to generalized social distancing measures. Quarantine can only apply to identified individuals, that is, symptomatic individuals. But there is reason to believe that with COVID-19 a large share of all infected are asymptomatic. In this case, it might be useful to identify and subsequently quarantine asymptomatic individuals through contact tracing and random testing.

Figure 2 provides a graphic representation of the model. Susceptible individuals, S, become exposed at the rate $\alpha I^*/N$, and exposed individuals, E, become infectious without symptoms, I_A, at the rate ϕ. Asymptomatic individuals recover at rate γ_A, and they become symptomatic at rate β. Symptomatic individuals, I_S, recover or die at rates γ_S and δ,

Figure 2: The Extended SEIR Model
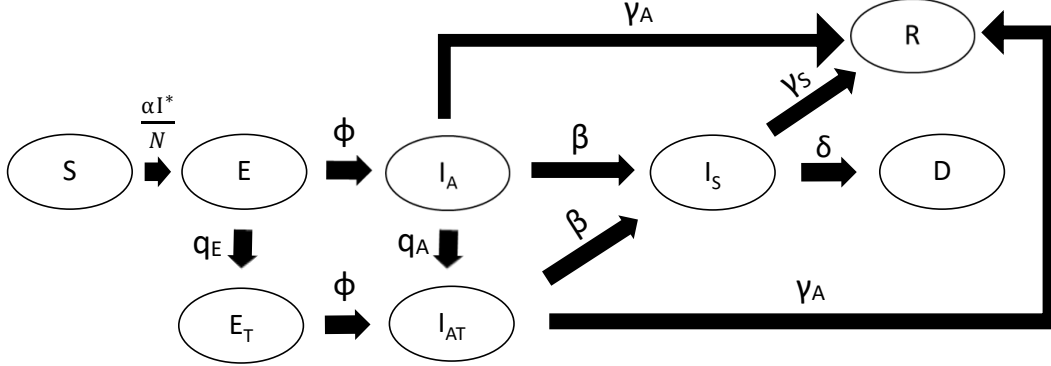
respectively.[2] The flow terms, q_E and q_A, and the stocks, E_T and I_{AT}, refer to the exposed and asymptomatic individuals who have been identified through tracing and/or random testing as discussed below.

The effects of policy interventions, such as social distancing and quarantining known infected individuals, are modeled through their impact on the flow of new infections. As in the basic SIR model, the flow of new infections is proportional to the product of susceptible individuals and infectious individuals, but quarantine can reduce the number of infectious individuals who can meet the susceptible population. We assume that symptomatic individuals are always known and that tracing and random testing can identify some exposed and asymptomatic individuals. Let ε_i denote the effectiveness of quarantine for the known infectious population groups, $i \in \{S, AT\}$, and also assume that asymptomatic infected are less infectious than symptomatic infected. The relative infectiousness of asymptomatic individuals is $\sigma \leq 1$. The effective pool of infectious individuals who meet the susceptible population and the inflow of newly infected individuals, I^* and M, respectively, are[3]

$$I^* = \sigma \left[I_A + (1 - \varepsilon_{AT}) I_{AT} \right] + (1 - \varepsilon_S) I_S, \tag{7}$$

$$M = \alpha S I^* / N. \tag{8}$$

---

[2]Total deaths are small enough such that the implicit assumption of a constant population is not too distorting.

[3]This version of targeted quarantine deviates from the standard model used in the epidemiological literature in the sense that identified people are added instantaneously to the quarantine pool, but some infections seep out of that pool. The epidemiological literature I am aware of assumes that infected individuals join the quarantine pool gradually following a Poisson process, but then quarantine is perfect. For example, Feng (2007).

The following system of differential equations provides the formal representation of the process dynamics.

$$\dot{S} = -M, \tag{9}$$

$$\dot{E} = M - \phi E - q_E, \tag{10}$$

$$\dot{I}_A = \phi E - (\beta + \gamma_A) I_A - q_A, \tag{11}$$

$$\dot{E}_T = q_E - \phi E_T, \tag{12}$$

$$\dot{I}_{AT} = q_A + \phi E_T - (\beta + \gamma_A) I_{AT}, \tag{13}$$

$$\dot{I}_S = \beta(I_A + I_{AT}) - (\gamma_S + \delta)I_S, \tag{14}$$

$$\dot{R} = \gamma_A (I_A + I_{AT}) + \gamma_S I_S, \tag{15}$$

$$\dot{D} = \delta I_S. \tag{16}$$

Since the cumulative number of deaths remains sufficiently small for our analysis, we ignore the impact of deaths on the surviving population in equation (8) to keep things simple.

Social distancing is assumed to directly reduce the rate at which individuals, infectious and susceptible, contact each other. We assume that the transmission rate can be split in two components: the contact rate for an individual, c, that captures social distancing interventions and individual responses to the spread of the disease, and a residual term, ψ, that captures all other disease-related features of transmission and non-pharmaceutical interventions. Then the transmission rate is

$$\alpha = (c\psi)^2. \tag{17}$$

Social distancing is thus potentially a very effective way to contain the spread of the disease since a reduction of contact rates applies to all individuals, infectious and non-infectious. Therefore, a reduction of contact rates implies a squared reduction of transmission rates. Social distancing is also "easy" to implement since all individuals are supposed to reduce their contact rates, that is, no particular information is required. This indiscriminate reduction of contact rates also makes social distancing very disruptive for the economy.

Quarantine methods, on the other hand, target individuals who are infectious, that is, they require information on an individual's health status. As long as the health status is observable, that is, for symptomatic individuals, it is relatively straightforward to implement, though not without cost. The problem with a disease like COVID-19 is that a large share of infectious individuals—current estimates are around 50 percent—may never show symptoms. Thus, even if one were to quarantine all symptomatic individuals, the pool of infectious individuals would be reduced by only half. On the other hand, quarantine is somewhat more efficient than that since symptomatic individuals are more infectious than asymptomatic

individuals. Contact tracing and random testing are attempts to reduce the pool of infectious individuals by quarantining asymptomatic individuals.

Tracing of asymptomatic infected individuals is modeled as follows. We assume that at the time an asymptomatic individual becomes symptomatic, a fraction ε_T of the people who this individual has infected and who are still in the exposed or asymptomatic state are traced.[4] The inflow into the pool of identified exposed and asymptomatic individuals is then

$$q_{TE} = \varepsilon_T \mathcal{R}_{ATE} \beta I_A \text{ and } q_{TA} = \varepsilon_T \mathcal{R}_{ATA} \beta I_A. \tag{18}$$

In appendix A.2 we show that

$$\mathcal{R}_{ATE} = \alpha \frac{S}{N} \frac{\sigma\beta}{(\beta + \gamma_A)(\beta + \gamma_A + \phi)}, \tag{19}$$

$$\mathcal{R}_{ATA} = \alpha \frac{S}{N} \frac{\sigma\beta\phi}{2(\beta + \gamma_A)^2(\beta + \gamma_A + \phi)}. \tag{20}$$

Testing is modeled as follows. Let fN be the flow rate at which not yet identified infected people are randomly tested. Assume that asymptomatic infected can be identified through tests but not merely exposed individuals. Also assume that recovered individuals are not tested. Then the share of identified asymptomatic in a random test is[5]

$$p_F = \frac{I_A}{S + E + I_A}. \tag{21}$$

The inflow of newly identified exposed and asymptomatic individuals through random testing is

$$q_{FE} = \varepsilon_T \mathcal{R}_{ATE} p_F fN \text{ and } q_{FA} = (1 + \varepsilon_T \mathcal{R}_{ATA}) p_F fN, \tag{22}$$

where we allow for the possibility that previous contacts of newly identified asymptomatic individuals are then also traced. Total inflows to the stock of identified exposed and asymptomatic individuals are

$$q_E = q_{TE} + q_{FE} \text{ and } q_{AT} = q_{TA} + q_{FA}. \tag{23}$$

4   Accounting for the pandemic

I now use a quantitative version of the extended SEIR model to account for the spread of the pandemic in the United States. First, I calibrate the parameters of the SEIR model

---

[4]We essentially assume that tracing does not require time but is instantaneous. It is straightforward to introduce a time delay for the recovery of tracked individuals. Again, we model the effectiveness of tracing not through the rate at which potentially traceable individuals enter the quarantine pool, but through the size of the captured pool, see footnote 3.

[5]This potentially overstates the effectiveness of random testing with incomplete quarantine to the extent that the infectious pool also contains symptomatic individuals.

based on available evidence on how COVID-19 spreads in the population. Then, I use the parametric model to infer the path of the transmission rate from observations of smoothed daily death rates.

4.1 Calibration

I select the model parameters based on three surveys of the epidemiological profile of COVID-19: the fact sheet posted by the Robert Koch Institut (RKI), and the summary of evidence in Ferguson et al. (2020) (F) and in Bar-On, Flamholz, Phillips and Milo (2020) (B).[6] References to the surveys cover either the surveys' summary of the literature or particular studies cited in the surveys.

- The latency period from infection to becoming infectious, $T_{E \to A}$, is about 3 days, (B).

- The incubation period from infection to the onset of symptoms, $T_{E \to S}$, is about 6 days, (RKI) and (F).

- There is a wide range of estimates for the prevalence of asymptomatic infections. (RKI) references studies that put the share of asymptomatic infections in a range from 20 percent to 90 percent.[7] (F) argues that 40 percent to 50 percent of infected are never identified, mainly because they are asymptomatic. We set the probability of never becoming symptomatic, $p_{A \to R}$, at 40 percent.

- The (RKI) suggests that contagiousness for light to moderate disease progression declines after 10 days, (F) puts it at 6.5 days, and (B) at 3.5 days. We set the average duration of infectiousness, T_{AS}, at 8 days.

- The infection fatality rate (IFR) is not well estimated, (B) puts in a range between 0.3 percent and 1.3 percent. We assume it to be $p_{AD} = 0.01$.

- Asymptomatic infections are between 30 percent (F) and 40 percent (RKI) less infectious than symptomatic infections. We set $\sigma = 0.6$.

- As for the effectiveness of quarantine, (F) assumes that two-thirds of symptomatic individuals self-isolate after one day. Since our quarantine does not involve any time delay, we assume that the baseline quarantine effectiveness, ε_S, is 50 percent.

---

[6]The RKI COVID-19 fact sheet is available at
https://www.rki.de/DE/Content/InfAZ/N/Neuartiges_Coronavirus/Steckbrief.html.
[7]The lower bound is based on a meta study of at-risk population groups, and the upper bound is based on serological studies that test for the presence of coronavirus antibodies in population samples.

In appendix A.1, we derive the average latency period, incubation period, duration of infectiousness, recovery probability from an asymptomatic infection, and IFR:

$$T_{E \to A} = \frac{1}{\phi} \tag{24}$$

$$T_{E \to S} = \frac{1}{\phi} + \frac{1}{\beta + \gamma_A} \tag{25}$$

$$p_{A \to R} = \frac{\gamma_A}{\gamma_A + \beta} \tag{26}$$

$$T_{AS} = \frac{1}{\beta + \gamma_A} \left(1 + \frac{\beta}{\gamma_S + \delta} \right) \tag{27}$$

$$p_{E \to D} = \frac{\beta}{\beta + \gamma_A} \frac{\delta}{\delta + \gamma_S}. \tag{28}$$

We infer the parameters (ϕ, γ_A, β) from $(T_{E \to A}, T_{E \to S}, p_{A \to R})$ using equations (24), (25), and (26). The remaining parameters (δ, γ_S) follow from $(T_{AS}, p_{E \to D})$ using equations (27) and (28). Table 1 summarizes the implied parameter values and observations used in their derivation.

Table 1: Baseline Calibration

Observation		Parameter	
T_E	= 3 days	ϕ	= 0.33
$T_{E \to S}$	= 6 days	γ_A	= 0.13
$p_{A \to R}$	= 40%	β	= 0.20
T_{AS}	= 8 days	γ_S	= 0.12
$p_{E \to D}$	= 1%	δ	= 0.0020

Finally, we note that we have not used two pieces of information from (RKI) in our calibration of the disease process. First, asymptomatic individuals cause about 45 percent of all infections. Second, 95 percent of individuals that eventually become symptomatic do so within 10-14 days. We can calculate these statistics for our calibration and find that they are quite close to the (RKI) statistics, 35 percent and 98 percent, respectively.

4.2 Inferred transmission rates

We now use the calibrated model to infer the transmission rate in the United States from the observed daily deaths for the period from March 2020 to December 2020. For this purpose, we assume that there is no contact tracing or random testing, that is, only symptomatic individuals are quarantined. From the flowchart of the model, Figure 2, we can see that in this case, there is a singular flow from exposure to death. This means that we can work

Figure 3: Daily Deaths
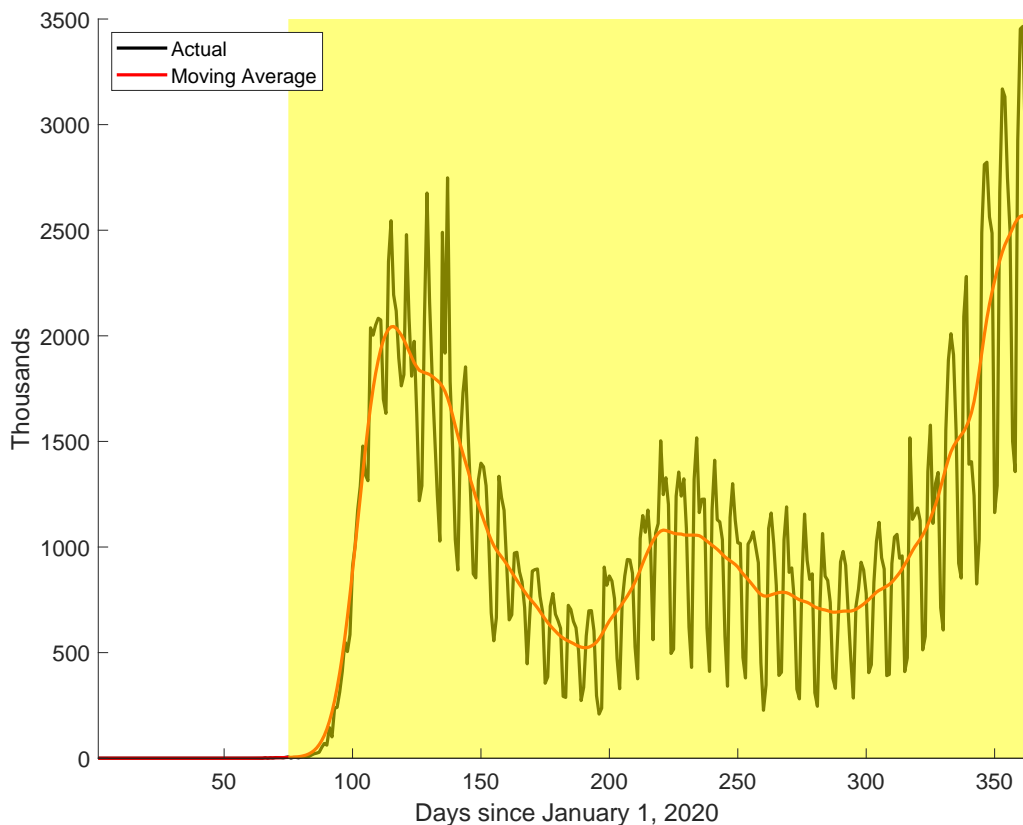
Note: The black line represents reported daily deaths, and the red line represents a Gaussian moving average of daily deaths with a symmetric forty-one-day window. The shaded area denotes the period after cumulative daily deaths exceed twenty-five.

our way backwards from daily deaths to initial infections that resulted in these deaths.[8] This is the approach Fernandez-Villaverde and Jones (2020) and Atkeson et al. (2020) use to estimate transmission rates and effective reproduction numbers.

In the online-only Technical Appendix to this paper, Hornstein (2021), we describe the algorithm that uses daily data on deaths to recover the stocks of preceding susceptible, exposed, and (a)symptomatic infectious individuals and the transmission rate. Suffice it to say that the stock of exposed individuals becomes a function of up to fourth order changes of daily deaths. This means that unless the path for daily deaths is very smooth, the inferred transmission rate will be exceedingly volatile and can be negative.

---

[8]Note that such a simple mechanical approach is not possible if daily deaths were the outcome of more than one distinct progression of the disease.

Actual daily deaths are extremely volatile—the black line in Figure 3—with a clear weekend seasonal in reported daily deaths. We therefore smooth the daily death data using a Gaussian moving average which filters out high frequency movements, the red line in Figure 3.[9]

We infer the transmission rate through the model's interpretation of smoothed observed daily deaths. The transmission rate is determined by the meetings of susceptible and infectious individuals, relative to the total size of the population. In the United States, as in most other countries, reported COVID-19-related deaths are concentrated in the adult population.[10] Furthermore, there is some evidence that younger children are less likely to transmit the coronavirus, e.g., Lewis (2020). Thus, an argument could be made to normalize the transmission rate with respect to the working age population. Qualitatively, the results do not depend on the normalization, but since the working age population is much smaller than the total population, the transmission rate inferred from the working age population measure is noticeably higher.[11] We follow the literature and use total population.

In Figure 4, we plot the log-level of the square root of the transmission rate, the black line.[12] The transmission rate declines rapidly in the first month after the first COVID-19-related deaths have been observed.[13] In particular, the transmission rate declines before California issues the first state wide stay-at-home order on March 19. The transmission rate precedes the path of daily deaths bottoming out in May, increasing again in the summer, declining in early fall, and then increasing in late fall and winter.

Associated with inferred transmission rates from daily deaths in Figure 4, are the time paths for the population shares of susceptible, exposed, (a)symptomatic individuals, cumulative deaths, and also the effective reproduction rate, the black lines in Figure 5. At its first peak in early April, about 0.5 percent of the population are infectious, Panels C&D, but that share declines relatively fast before it increases again in mid-summer and reaches a new higher peak in December. Given the calibration, at any point in time, somewhat less than half of infectious individuals are asymptomatic, Panel C, and about one-fourth of infected individuals are not yet infectious, Panel B. Associated with the transmission rate is the effective reproduction number in Panel F. The reproduction number is initially quite high,

---

[9]To be precise, we use the MATLAB routine `smoothdata` with the `gaussian` option and a symmetric thirty-one-day window. Essentially, the Gaussian moving average is a moving average with weights that correspond to a normal probability density function.

[10]As of January 2021, more than 99.8 percent of all deaths are among those 17 years and older. See https://covid.cdc.gov/covid-data-tracker/#demographics. Accessed 1/6/2021.

[11]The Census estimates U.S. working age population, that is, those aged 16 and older, to be 263.5 million, as opposed to a total population of 329.5 million.

[12]We plot the transmission rate for the period once cumulative deaths exceed twenty-five. Prior to that, the inferred transmission rate tends to be very large and volatile, even using smoothed daily deaths.

[13]A point emphasized by Atkeson et al. (2020).

Figure 4: Transmission Rate
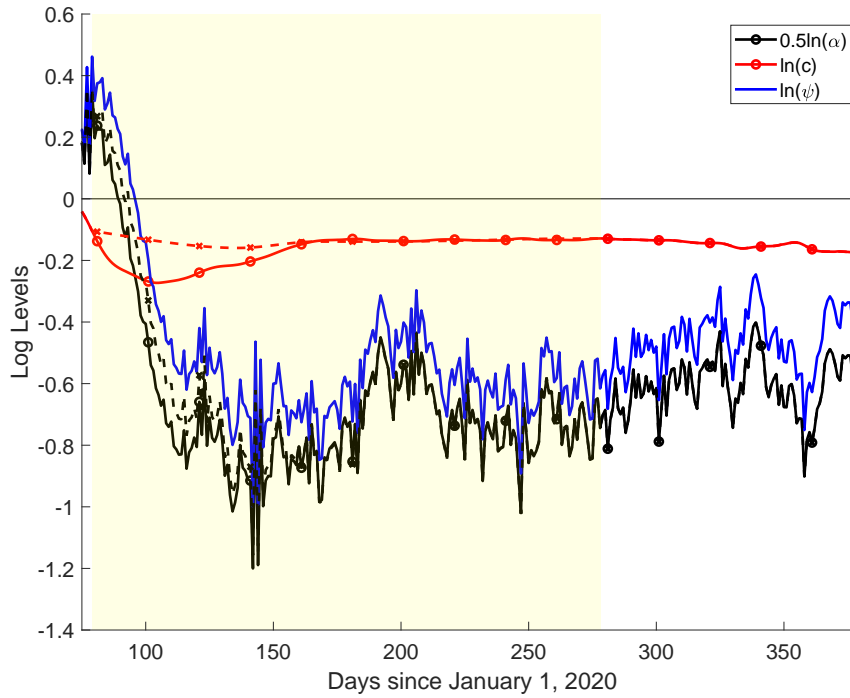
Note: The solid black line represents the inferred transmission rate, $0.5 \ln \alpha$, the solid red line represents the aggregate measured contact rate, $\ln c$, and the solid blue line represents the residual component, $\ln \psi$. All rates are in log levels. The red and black dashed lines represent the alternative measured contact and transmission rates based on the alternative employment rate. The shaded area denotes the period for which the hypothetical alternative employment rate deviates from the actual employment rate. The left-hand side boundary of the shaded area is the seventy-ninth day of the year, March 19, and the right-hand side boundary is the 278 day of the year, October 4.

above four, but rapidly declines to values below two in April and then fluctuates between 0.5 and two for the rest of the year, being elevated toward the end of the year when infections and deaths are increasing. At the end of the year, cumulative deaths make up about 0.095 percent of the population.

5 Experiments

Various measures affect the transmission rate of COVID-19 and the way the pandemic spreads: from simple non-pharmaceutical interventions, such as hand washing and wearing face masks, to extended social distancing measures, such as scaling back certain economic activities. This section uses the previously derived framework to focus on the effects of the sharp reduction in employment in spring 2020 and possible alternatives to this approach. For this purpose, we first construct a simple model that maps employment and other social interactions into an aggregate contact rate. We then remove the aggregate contact rate from the inferred transmission rate and obtain a residual transmission rate. By construction, the residual transmission rate captures all other social distancing measures and non-pharmaceutical interventions in addition to disease-related characteristics that are not captured by the aggregate contact rate. We then replace the observed employment decline with an alternative employment path that converges gradually to the levels of fall 2020 employment and avoids the sharp decline and recovery in the spring and summer. Obviously, the increased contact rates from this alternative employment path would have increased fatalities. Then, we ask what alternative quarantine policy could have contained fatalities. Finally, we ask if contact tracing or random testing could have improved on this outcome.

While the construction of our counterfactual experiments is straightforward, there is an obvious qualification to the results we obtain. We are combining the counterfactual paths for work contacts and COVID-19 containment policies with the residual transmission rate path, but the latter incorporates behavioral responses to the actual path of fatalities. To the extent that our experiments yield different paths for fatalities, one would expect that residual contact rates change. In particular, the endogenous response of contact rates would dampen the impact on fatalities in the counterfactual.

5.1 Measured contact rates

How much of the observed variation in transmission rates can we attribute to measured variations of contact rates, in particular, contact rates related to employment? To answer this question, we construct an index that aggregates information on employment and mobility indices. Our approach is a simplified version of Baqaee et al. (2020).

Figure 5: Policy Interventions
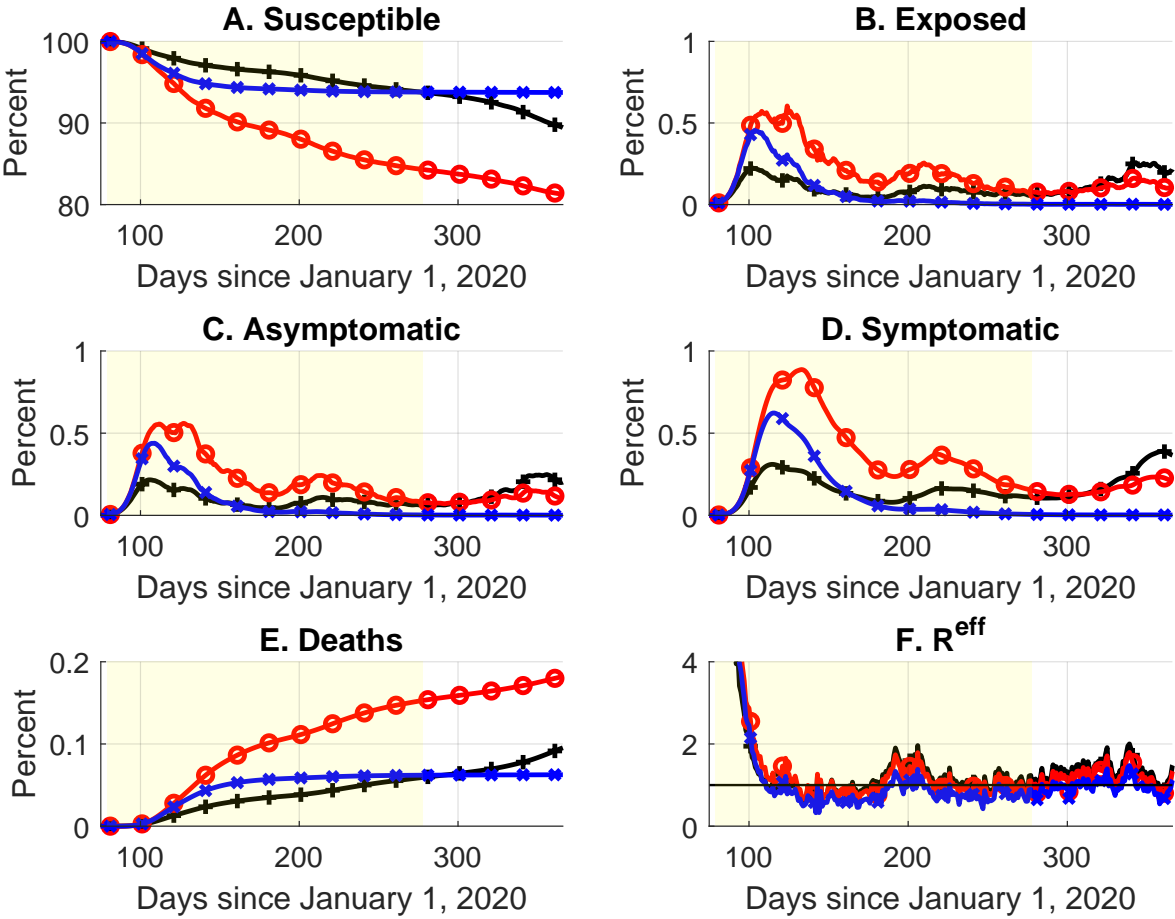
Note: The black lines represent the baseline outcome using the inferred transmission rate. The red lines represent the outcome for the alternative transmission rate and no change in quarantine effectiveness, $\epsilon_S = 0.5$. The blue lines represent the outcome for the alternative transmission rate and increased quarantine effectiveness, $\epsilon_S = 0.7$. The shaded area denotes the period for which the alternative transmission rate deviates from the inferred transmission rate, see notes to Figure 4.

We first construct work-related contacts from monthly payroll employment data and the Bick et al. (2021) survey of workplace locations. Based on survey data that are patterned on the monthly CPS, Bick et al. (2021) argue that the share of the U.S. workforce that is working from home increased from about 8 percent in February 2020 to about 30 percent in May 2020 and then declined to about 20 percent in the fall.[14] We define work contacts as the product of payroll employment and the share of those working away from home. Essentially, we assume that different contact rates apply to those working at home and those working away from home.

The employment series and the share of those working away from home are plotted in Figure 6.a.[15] Despite the large decline of employment early in the pandemic, about 15 percent at its trough in April, the 25 percent decline of those working away from home dominates the decline in work contacts. Work contacts decline persistently over the year by 20 percent, two-thirds due to the decline in the share of those working away from home.

We combine the work contact index with a social contact index related to non-work activities away from home by aggregating Google mobility indices for shopping and recreation activities.[16] Social contacts started to increase in early March but then dropped off sharply, preceding the drop-off in work contacts by about a week, Figure 6.b. These social contacts recovered somewhat faster than work contacts in the summer, but they also did not return to their pre-pandemic levels, and they declined in the fall when daily deaths started to increase again.

Aggregate contacts are defined as the sum of contacts from three activities, 'Home' (H), 'Work' (W), and 'Social' (S),

$$c_t = \sum_{i \in \{H,S,W\}} x_t^i c^i, \tag{29}$$

with fixed weights, c^i, and the normalized social and work indices as activity measures relative to pre-pandemic levels, x_t^i. Home contacts are fixed at one, $x_t^H = 1$.

We obtain the contact weights from a survey on social contacts in Europe.[17] Mossong et al. (2008), Figure 2, display the average distribution of contacts for the pool of all countries.

---

[14]Parker, Horowitz and Minkin (2020) report a similar pattern in Pew survey data.

[15]We interpolate the two monthly series using piece-wise cubic splines and normalize each series at one on February 15, 2020.

[16]We average the daily Google mobility indices starting February 15 for Retail and Recreation locations, Grocery and Pharmacy locations, and Transit Stations. We then calculate a seven-day moving average of the average Google index and normalize the series to one on February 15.

[17]The survey covers eight European countries in 2005 and 2006. The purpose of the study was to "determine patterns of person-to-person contact relevant to controlling pathogens spread by respiratory or close-contact routes," Mossong, Hens, Jit, Beutels, Auranen, Mikolajczyk, Massari, Salmaso, Tomba, Wallinga, Heijne, Sadkowska-Todys, Rosinska and Edmunds (2008).

Roughly, the allocation of contacts among activities is: 'Other' 15 percent, 'Leisure' 15 percent, 'School' 12 percent, 'Home' 25 percent, 'Work' 20 percent, 'Multiple' 8 percent, and 'Transport' 5 percent. We drop 'School' contacts and combine all other groups except 'Home' and 'Work' into 'Social', now 35 percent. That leaves us with 25 percent H, 20 percent W, and 35 percent S, and we re-normalize the weights so that they add up to one.

The aggregate contact index is displayed as the red line in Figure 6.b. Since constant home contacts receive a weight of one-third in our weighting scheme, aggregate contacts do not fall as much as either work or social contacts.

We now split the transmission rate into a part that is due to the measured contact rates and an unexplained residual term, ψ,

$$0.5 \ln \alpha = \ln c + \ln \psi, \tag{30}$$

the red and blue lines in Figure 4, respectively. According to this procedure, the impact of reduced social contacts and employment on the transmission rate is limited: changes in these contacts account for about one-third of the decline in the overall transmission rate. We will now use our calibrated model to study what could have happened if social distancing policies had been less restrictive and had been accompanied by other non-pharmaceutical interventions such as efficient quarantine, contact tracing, or random testing.

5.2 Alternative employment path

We take the sharp decline of employment in March and April, followed by a partial recovery by October, as the main employment impact of stay-at-home orders. Taking the partial recovery by the fall as given, we essentially assume that many of the employment losses in the hospitality and recreation sector were unavoidable without a vaccine.

The alternative employment path we propose has employment gradually converge to its fall 2020 values, starting in mid-March, the dashed purple line in Figure 6.a.[18] Since social contacts are correlated with market activity, we assume that social contacts follow a similar path, with the same beginning and end points, the dashed cyan line in Figure 6.b. Combining the time paths for work and social contacts yields the aggregate contact index, the dashed red line in Figure 6.b. Combining the alternative contact index with the residual transmission rate we now have the transmission rate, associated with the alternative employment path, the dashed red and black lines, respectively, in Figure 4.

Avoiding the sharp decline in employment doubles the eventual fatalities in the calibrated model. The red lines in Figure 5 plot the time paths for the population shares of susceptible,

---

[18]The alternative employment path is a cubic spline that connects March 19, when California issued the first statewide stay-at-home order, with October 4, when employment has apparently stabilized.

Figure 6: Measured Contact Rates
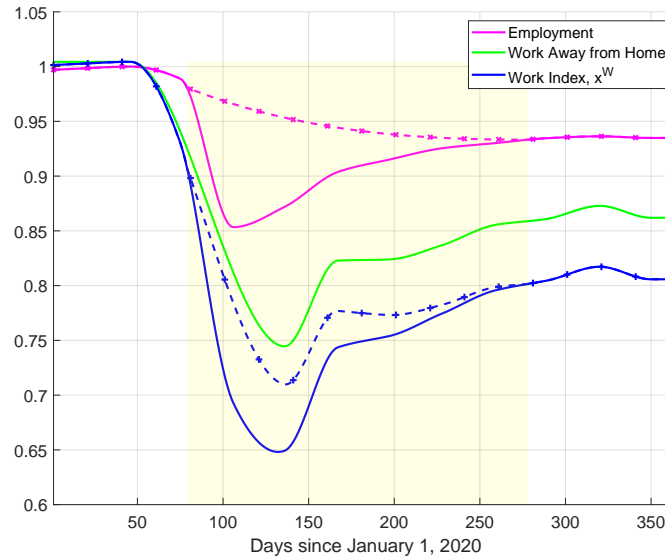
(a) Work Contacts
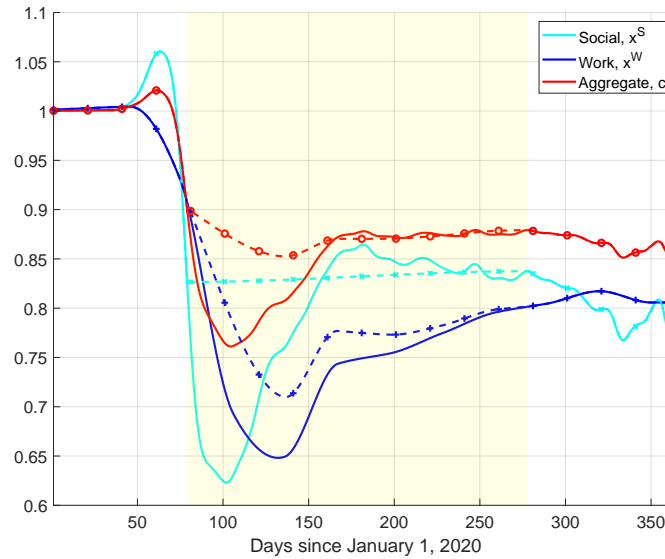
(b) Aggregate Contacts

Note: In Panel (a), the purple line is total nonfarm payroll employment, the green line is the fraction of those employed that are working away from home, and the blue line is employment away from home, also in Panel (b). In Panel (b), the magenta line is social contacts not at home and not at work, and the red line is an index of all contacts. All series are normalized to one on February 15, 2020. The construction of the contacts is described in the text. The solid lines represent observed variations in contacts, and the dashed lines represent hypothetical time paths for contacts as described in the text. The shaded area highlights the time period for which the hypothetical contacts deviate from actual contacts.

19

exposed, and (a)symptomatic individuals, and cumulative deaths for the transmission rates implied by the alternative employment path. The number of infectious individuals on the alternative path more than triples relative to the baseline path and so do cumulative deaths during the time the alternative path deviates from the baseline path. Because there are so many more infections on the alternative path, the population share of susceptible individuals declines to about 80 percent, as opposed to staying above 90 percent for the baseline path. Fewer susceptible individuals then means lower effective reproduction rates at the end of the year and fewer additional infections and deaths. Nevertheless, cumulative deaths at the end of the year make up about 0.19 percent of the population, twice the number actually realized.

5.3 Alternative policies: quarantine, contact tracing, testing

We now consider three alternative policies that might be put in place for the alternative employment path: more efficient quarantine, contact tracing, and finally random testing. Increased quarantine effectiveness keeps cumulative fatalities low in the longer run, although in the short run, fatalities increase faster than in the baseline case. Contact tracing reduces fatalities somewhat, but the reductions, even from a perfectly effective contact tracing scheme, are limited when combined with a more effective quarantine program. Finally, the reductions of fatalities from even large-scale random testing programs are limited.[19]

5.3.1 Quarantine

Quarantine is assumed to be 50 percent effective in our baseline calibration, that is, half of symptomatic individuals are assumed to (self)quarantine. We now consider the case when quarantine effectiveness is permanently increased to 70 percent for the alternative employment path.

A more efficient permanent quarantine regime does not prevent the increase of fatalities relative to the baseline case in the short run, but it substantially reduces cumulative fatalities in the long run. The blue lines in Figure 5 plot the time paths for the population shares of susceptible, exposed, and (a)symptomatic individuals, and cumulative deaths for the transmission rates implied by increased quarantine for the alternative employment path. With the higher quarantine effectiveness, the number of infectious individuals now only doubles relative to the baseline path for the first thirty days, and so do cumulative deaths. But after seventy days, the number of infectious individuals is less than in the baseline case, and cumulative deaths level out. In fact, with the higher permanent quarantine rate, the

---

[19]For each policy parameter, we consider a permanent increase from the baseline calibration value to its alternative value. We assume that the increase is spread out over forty days, starting March 19, 2020.

Table 2: Effectiveness of Quarantine, Tracing, and Random Testing

ε_Q	(1)	(2)	(3)	(4)	(5)	(6)	(7)	(8)
			ε_T				f	
	0.000	0.250	0.500	0.750	1.000	0.001	0.010	0.100
0.500	0.187	0.181	0.176	0.171	0.166	0.153	0.148	0.110
0.600	0.101	0.097	0.094	0.090	0.087	0.071	0.069	0.054
0.700	0.063	0.060	0.058	0.057	0.055	0.042	0.041	0.034
0.800	0.044	0.043	0.041	0.040	0.039	0.029	0.028	0.024
0.900	0.033	0.032	0.031	0.030	0.029	0.022	0.021	0.018
1.000	0.026	0.025	0.024	0.024	0.023	0.017	0.016	0.014

Note: Cumulative deaths at end of sample, December 31, 2020, as a percent of population for given alternative transmission path and variations of quarantine effectiveness, ε_Q, tracing effectiveness, ε_T, and testing rate, f. Rows represent different values of the common quarantine effectiveness, $\varepsilon_Q = \varepsilon_S = \varepsilon_{AT}$. Columns 1 through 5 represent variations of the tracing effectiveness parameter in the absence of random testing, $f = 0$. Columns 6 through 8 represent variations of the testing rate for a fixed tracing effectiveness, $\varepsilon_T = 0.5$. The testing rate f denotes the daily fraction of population that is randomly selected for testing.

pool of infected individuals becomes so small that infections are not increasing in the late fall as the transmission rate and the effective reproduction number is increasing again.

Increasing quarantine effectiveness permanently from 50 percent to 70 percent reduces cumulative deaths on the alternative employment path at the end of the year by two-thirds, Table 2, column 1. This represents about two-thirds of the cumulative deaths on the baseline path, and most of that reduction is attained at the end of the year when increased quarantine effectiveness contains the spike in transmission rates. But even a more limited permanent increase of quarantine effectiveness to 60 percent contains cumulative deaths on the alternative employment path at the same level as the baseline path. Increasing quarantine effectiveness beyond 70 percent further reduces cumulative deaths at a diminishing rate.

5.3.2 Contact tracing

Contact tracing, as defined in equations (19) and (20), is assumed to instantaneously identify and quarantine a fraction of the individuals who a newly symptomatic individual has infected. It follows that contact tracing can only be effective as long as quarantine is effective.

Our model suggests that the reductions of cumulative deaths from contact tracing are limited, even though about half of infectious individuals are asymptomatic. We display end-of-year cumulative deaths for various combinations of quarantine and contact tracing

efficiencies in Table 2, columns 1 through 5.[20] As we can see, the most that contact tracing can achieve, if it is perfectly efficient, is to reduce cumulative deaths by about 10 percent for any level of quarantine effectiveness considered. Contact tracing that quarantines half of the identified infected individuals reduces cumulative deaths by about 5 percent.

In our environment, even perfect contact tracing captures only a small fraction of the asymptomatic infectious individuals. Figure 7 replicates Figure 5 for the alternative employment path with more effective quarantine, $\varepsilon_S = 0.7$, without and with perfect contact tracing, $\varepsilon_T = 0$ and 1. As we can see, only a small fraction of asymptomatic individuals, maybe a tenth, is identified and quarantined.

The reason why contact tracing has limited effects can be understood as follows. From equation (20) the maximal measure of asymptomatic individuals that can be traced from newly symptomatic individuals is

$$\mathcal{R}_{ATA}\beta I_A = \alpha \frac{S}{N} \frac{\sigma\beta}{(\beta + \gamma_A)(\beta + \gamma_A + \phi)}\beta I_A. \tag{31}$$

Compare this inflow into the pool of traced asymptomatic individuals with the inflow into the pool of asymptomatic individuals from new infections

$$\alpha \frac{S}{N} I^* \approx \alpha \frac{S}{N} \left[\sigma + (1 - \varepsilon_Q)\right] I_A, \tag{32}$$

where the approximation is based on about equal numbers of asymptomatic and symptomatic individuals.[21] From our calibration, the scale factors in equations (31) and (32) are 0.3 and 1.3, respectively. Thus, inflows into the pool of traced asymptomatic individuals are less than one-fourth of the inflows into the pool of asymptomatic individuals. Which explains why contact tracing, even in the best of cases, cannot track that many infected individuals.[22]

5.3.3 Testing

Early on in the pandemic, daily tests covered less than 0.05 percent of the population, but at the end of 2020, daily tests covered about 0.7 percent of the population. Within the framework of this paper, this ten-fold increase may attain most of the gains that could be obtained from random testing.[23]

---

[20]We assume that the quarantine effectiveness for traced asymptomatic and exposed individuals is the same as for symptomatic individuals.

[21]We have also ignored the time delay coming from the exposed state.

[22]In appendix A.4, we consider alternative calibrations that increase the share and the relative infectiousness of asymptomatic infectious individuals. Neither alternative calibration increases the effectiveness of contact tracing.

[23]We should note that throughout the pandemic, tests were predominately used for the confirmation of symptomatic cases or suspected infections, not random testing.

Figure 7: Contact Tracing
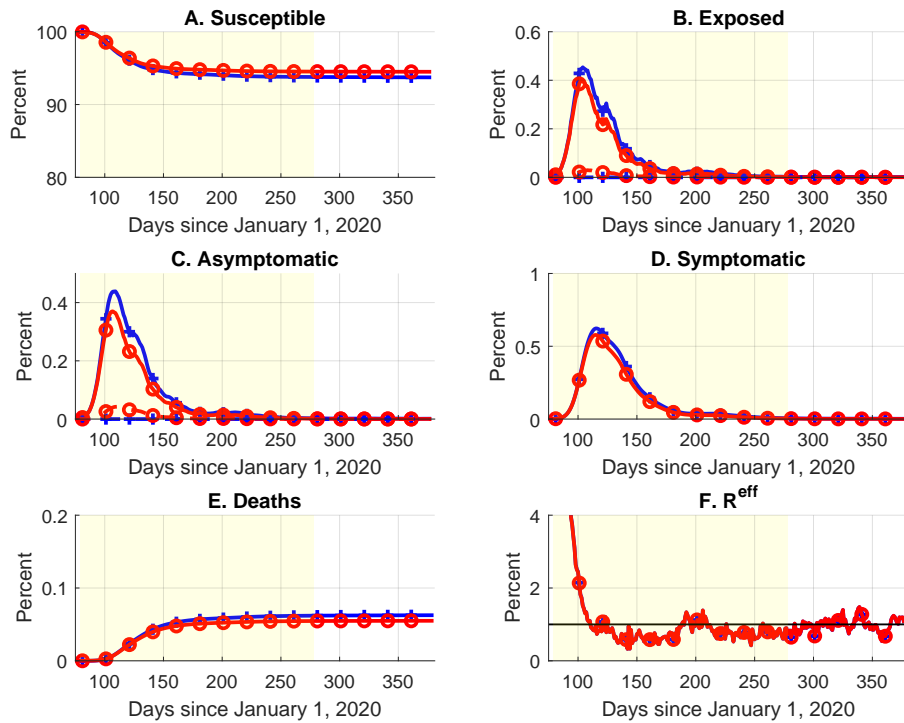
Note: The blue lines represent the outcome for the alternative transmission rate and increased quarantine effectiveness, $\varepsilon_S = 0.70$, but no contact tracing. The red lines represent the outcomes when perfectly effective contact tracing is added, $\varepsilon_T = 1.0$. The dashed lines in panels B and C represent the traced and quarantined asymptomatic individuals, and the solid lines represent the unidentified and not quarantined individuals.

In Table 2, columns 6 through 8, we display end-of-year cumulative deaths for various combinations of quarantine effectiveness and testing rate, given the alternative employment path and a 50 percent tracing effectiveness. Relative to no random tests, Table 2, column 5, randomly testing 0.1 percent of the population every day reduces cumulative deaths by one-fourth to one-third when quarantine effectiveness exceeds 70 percent. Increasing the daily testing rate to 1 percent of the population does not reduce cumulative deaths much more, but increasing the daily testing rate to 10 percent of the population cuts cumulative deaths in half relative to no testing.

5.4 The costs and benefits of alternative policies

Cutler and Summers (2020) have calculated the net-cost of COVID-19 from impaired health and lost lives and output at \$16.1 trillion, about 90 percent of 2019 GDP. We use their approach to calculate the benefits and costs of the alternative policies described in the previous section. We estimate the gains from increasing quarantine effectiveness to 70 percent, combined with a 50 percent effective contact tracing scheme and a daily testing of 1 percent of the population to be \$4.9 trillion, close to a quarter of 2019 GDP. Increasing the effectiveness of quarantine and contact tracing to 100 percent, if it was feasible, would result in additional net gains of \$2 trillion, another 9 percent of GDP. Almost all of the gains are associated with reductions in loss of life and improved health outcomes of survivors.

We estimate the GDP gains from the alternative employment path assuming that labor productivity on the alternative path is the same as on the actual path. We calculate the GDP gain as roughly half a trillion dollars, about 2.5 percent of 2019 GDP. Our procedure is likely to overstate the potential GDP gains from the alternative employment path since labor productivity increased substantially in the 2020 downturn: employment losses were concentrated in low productivity sectors, such as hospitality and leisure. As we now show, this is unlikely to matter much since benefits from improved health outcomes far outweigh the gains from increased GDP.

Greenstone and Nigam (2020) and Cutler and Summers (2020) use the VSL to evaluate the benefits from reduced mortality rates. The VSL represents a person's willingness to pay for a reduced probability of death and is a concept used by U.S. federal agencies to evaluate the benefits of policies. For example, the EPA uses an inflation adjusted 2020 VSL for an adult U.S. citizen of \$11.5 million (Greenstone and Nigam 2020, p. 14). I follow Cutler and Summers (2020), who on the one hand, use a more conservative estimate of \$7 million for the VSL, but on the other hand assume that for every death there are seven survivors who suffered severe infections, the negative health effects of which are equivalent to a 35 percent

24

reduction of their VSL. The net effect of these assumptions is that a death is valued at $24 million.

Finally, the assumptions on the cost of quarantine, contact tracing, and random testing are as follows. For quarantine, we assume that an identified infected individual is quarantined for two weeks and gets reimbursed for lost income and expenses. The average weekly income in the BLS Covered Employment and Wages for the first quarter of 2020 was $1,200, and we assume that a quarantined individual receives a weekly per diem of $1,000. Thus, the total cost per quarantined individual is $4,400.[24] Cutler and Summers (2020) assume that a contact tracing program would cost $25 billion, which we treat as a fixed cost, independent of how many cases will be traced.[25] We assume that the unit cost of a random test is $100.[26]

Table 3 restates the impact on cumulative deaths from alternative policies in Table 2 in terms of the benefits from improved health outcomes and the cost of attaining them. The first thing to notice is that the output gains from the alternative employment path are roughly one-tenth the value of the improved health outcomes for quarantine effectiveness at 70 percent or higher. Even if we did not consider permanent health damages to survivors of severe infections and scaled back the value of a death by two-thirds, improved health outcomes would still be twice as valuable than the gains from increased output. Second, the costs of attaining these outcomes are about a fourth of the increased output, and they are decreasing as quarantine effectiveness increases since the number of infected individuals who need to be quarantined declines. Third, even though reductions of cumulative deaths from contact tracing and random testing on top of effective quarantine are limited, the value gain from these reductions in deaths still exceeds the gains from increased output.

6   Conclusion

I have studied the effectiveness of alternative policies to contain the spread of a pandemic in a SEIR model that is calibrated to the characteristics of COVID-19. In particular, the model allows for asymptomatic infectious individuals, an approach that suggests the use of contact tracing, conditional on having an effective quarantine policy in place. When the model's disease transmission is matched to the 2020 U.S. experience, I find that permanent

---

[24]This cost does not include any resources used to verify that individuals indeed stay quarantined. On the other hand, we assume that all quarantined individuals receive the payment and not just the ones in excess of the baseline quarantine rate.

[25]This cost corresponds to scaled versions of the cost of contact tracing programs in South Korea and Taiwan.

[26]On October 15, 2020, the Centers for Medicare and Medicaid services announced that Medicare would reimburse high throughput COVID-19 tests at $100, https://www.cms.gov/newsroom/press-releases/cms-changes-medicare-payment-support-faster-covid-19-diagnostic-testing.

Table 3: Costs and Benefits of Alternative Policies

ε_Q	(1)	(2)	(3)	(4)	(5)	(6)	(7)	(8)
			ε_T				f	
	0.000	0.250	0.500	0.750	1.000	0.001	0.010	0.100
	A. GDP gain from alternative employment path, $ 0.509 Trillion							
	B. Benefit from improved health outcome, Trillions of $s							
0.500	-6.560	-6.093	-5.652	-5.236	-4.843	-3.850	-3.384	-0.409
0.600	0.290	0.594	0.872	1.127	1.362	2.668	2.863	4.049
0.700	3.332	3.505	3.662	3.807	3.941	4.986	5.068	5.616
0.800	4.790	4.906	5.013	5.112	5.203	6.004	6.051	6.388
0.900	5.657	5.744	5.824	5.899	5.967	6.595	6.627	6.860
1.000	6.237	6.306	6.369	6.427	6.481	6.985	7.008	7.178
	C. Cost of improved health outcome, Trillions of $s							
0.500	0.108	0.107	0.106	0.104	0.103	0.106	0.186	0.999
0.600	0.078	0.077	0.076	0.075	0.074	0.073	0.155	0.974
0.700	0.063	0.062	0.062	0.061	0.061	0.061	0.143	0.965
0.800	0.056	0.055	0.055	0.055	0.054	0.056	0.138	0.961
0.900	0.051	0.051	0.050	0.050	0.050	0.052	0.134	0.958
1.000	0.048	0.047	0.047	0.047	0.046	0.050	0.132	0.956

Note: This table displays the benefits and costs associated with the alternative policies considered in Table 2. Panel A displays the GDP gains from the alternative employment path, Panel B displays the benefits from reduced cumulative deaths and other COVID-19-related health outcomes, and Panel C displays the costs associated with the quarantine, tracing, and testing programs as described in the text.

improvements of quarantine effectiveness, together with contact tracing and possibly random testing, can substantially lower cumulative deaths. These policies contain fatalities, even for an alternative employment path that avoids the sharp drop in March and April 2020.

Using standard VSL assumptions, we show that the gains from reduced fatalities could be up to one third of GDP, an order of magnitude larger than the gains from improved employment outcomes and the potential fiscal costs of the programs. We have not tried to find an optimal policy, but the results from our more limited analysis suggest that if such an analysis were to use standard VSL for fatalities, the reduction of fatalities rather than the containment of output losses would likely be the primary objective.

We should qualify the statement on the potential gains from these policies for at least two reasons. First, apart from the proposed changes in employment paths, we assume that any other behavioral responses to the pandemic remain unchanged. For example, if in our simulations, alternative policies reduce cumulative deaths, individuals are assumed not to let down their guard and return to their previous pattern of social interaction. Second, we have not considered the potentially large losses due to the disruptions of schooling. For example, Fernald, Li and Ochse (2021) argue that reduced educational attainment due to the pandemic can lower the level of GDP by up to 0.5 percentage points for the next sixty years. If we use a one percent discount rate, that would mean a 15 percent reduction in the present value of GDP, which is large but still only half of the potential benefits from reduced fatalities.

References

Atkeson, Andrew G., Karen Kopecky, and Tao Zha, "Estimating and Forecasting Disease Scenarios for COVID-19 with an SIR Model," Technical Report June 2020.

Baqaee, David, Emmanuel Farhi, Michael Mina, and James H. Stock, "Policies for a Second Wave," *Brookings Papers on Economic Activity*, Summer 2020.

Bar-On, Yinon M., Avi Flamholz, Rob Phillips, and Ron Milo, "SARS-CoV-2 (COVID-19) by the numbers," *eLife*, March 2020.

Berger, David, Kyle Herkenhoff, Chengdai Huang, and Simon Mongey, "Testing and Reopening in an SEIR Model," *Review of Economic Dynamcis (forthcoming)*, 2021.

Bick, Alexander, Adam Blandin, and Karel Mertens, "Work from Home Before and After the COVID-19 Outbreak," Technical Report 2017, Federal Reserve Bank of Dallas February 2021.

Cutler, David M. and Lawrence H. Summers, "The COVID-19 Pandemic and the $16 Trillion Virus," *JAMA*, 10 2020.

Feng, Zhilan, "Final and Peak Epidemic Sizes for SEIR Models with Quarantine and Isolation," *Mathematical Biosciences and Engineering*, 2007, *4*, 675–686.

Ferguson, Neil M. et al., "Impact of Non-Pharmaceutical Interventions (NPIs) to Reduce COVID-19 Mortality and Healthcare Demand," Technical Report 2020.

Fernald, John, Huiyu Li, and Mitchell Ochse, "Future Output Loss from COVID-Induced School Closures," *FRBSF Economic Letter*, February 2021.

Fernandez-Villaverde, Jesus and Charles Jones, "Estimating and Simulating a SIRD Model of COVID-19 for Many Countries, States, and Cities," *Working Paper*, May 2020.

Greenstone, Michael and Vishan Nigam, "Does Social Distancing Matter?," *Covid Economics, Vetted and Real-Time Papers*, April 2020, pp. 1–23.

Hornstein, Andreas, "Social Distancing, Quarantine, Contact Tracing, and Testing: Implications of an Augmented SEIR Model," *Covid Economics, Vetted and Real-Time Papers*, May 2020, pp. 42–72.

——— , "Technical Appendix for *Quarantine, Contact Tracing, and Testing: Implications of an Augmented SEIR Model*," Technical Report 2021.

Jewell, Nicholas P., Joseph A. Lewnard, and Britta L. Jewell, "Predictive Mathematical Models of the COVID-19 Pandemic: Underlying Principles and Value of Projections," *JAMA*, April 2020.

Lewis, Dyani, "Why Schools Probably Aren't COVID Hotspots," *Nature*, October 2020, *17*.

Lipsitch, Marc et al., "Transmission Dynamics and Control of Severe Acute Respiratory Syndrome," *Science*, 2003, *300* (5627), 1966–1970.

Mossong, Joël, Niel Hens, Mark Jit, Philippe Beutels, Kari Auranen, Rafael Mikolajczyk, Marco Massari, Stefania Salmaso, Gianpaolo Scalia Tomba, Jacco Wallinga, Janneke Heijne, Malgorzata Sadkowska-Todys, Magdalena Rosinska, and W. John Edmunds, "Social Contacts and Mixing Patterns Relevant to the Spread of Infectious Diseases," *PLOS Medicine*, 3 2008, *5* (3).

Parker, Kim, Julia Horowitz, and Rachel Minkin, "How the Coronavirus Outbreak Has – and Hasn't – Changed the Way Americans Work," Technical Report December 2020.

Piguillem, Facundo and Liyan Shi, "Optimal COVID-19 Quarantine and Testing Policies," EIEF Working Papers Series 2004, Einaudi Institute for Economics and Finance (EIEF) 2020.

Wearing, Helen J., Pejman Rohani, and Matt J. Keeling, "Appropriate Models for the Management of Infectious Diseases," *PLOS Medicine*, July 2005, *2* (7).

A Appendix

Detailed derivations for the statistics defined in this appendix can be found in the online-only Technical Appendix to this paper, Hornstein (2021).

A.1 Calibration

Here we define certain statistics that are used in the calibration of the model.

The probability that an exposed individual eventually becomes symptomatic is

$$p_{E \to S} = \int_0^\infty \left\{ \int_0^\tau \left[\phi e^{-\phi s} \right] \left[\beta e^{-\beta(\tau-s)} \right] \left[e^{-\gamma_A(\tau-s)} \right] ds \right\} d\tau,$$

where the first term is the probability that the individual becomes asymptomatic infectious at s and then becomes symptomatic at τ, without recovering. This can be solved as

$$p_{E \to S} = \frac{\beta}{\gamma_A + \beta}. \tag{A.1}$$

The average time for an exposed individual to become symptomatic, conditional on eventually becoming symptomatic, is

$$T_{E \to S} = \int_0^\infty \tau \left\{ \int_0^\tau \frac{\left[\phi e^{-\phi s} \right] \left[\beta e^{-\beta(\tau-s)} \right] \left[e^{-\gamma_A(\tau-s)} \right]}{p_{E \to S}} ds \right\} d\tau,$$

where the term in curly brackets is the probability of becoming symptomatic at τ, conditional on eventually becoming symptomatic. This can be solved as

$$T_{E \to S} = \frac{1}{\phi} + \frac{1}{\gamma_A + \beta}. \tag{25}$$

Note that this can be rewritten as

$$T_{E \to S} = \frac{1}{\phi} + \frac{\beta}{\gamma_A + \beta} \frac{1}{\beta} = T_E + p_{A \to S} T_{A \to S} = T_E + T_A,$$

where the first term is the average time spent being latent, and the second term is the probability of becoming symptomatic times the average time it takes to become symptomatic from asymptomatic.

The probabilities that an infected individual becomes symptomatic or recovers before becoming symptomatic are

$$p_{A \to S} = \frac{\beta}{\gamma_A + \beta} \tag{A.2}$$

$$p_{A \to R} = \frac{\gamma_A}{\gamma_A + \beta}. \tag{26}$$

The average duration of infectiousness, that is, the average time spent in states A and S is

$$T_{AS} = \int_0^\infty \left\{ \tau \left[\gamma_A e^{-\gamma_A \tau} \right] \left[e^{-\beta \tau} \right] + \left(\tau + \frac{1}{\gamma_S + \delta} \right) \left[e^{-\gamma_A \tau} \right] \left[\beta e^{-\beta \tau} \right] \right\} d\tau,$$

where the first term in the integral represents being asymptomatic for duration τ, followed by a recovery, and the second term of the integral represents being asymptomatic for duration τ, followed by being symptomatic with an average duration $1/(\gamma_S + \delta)$. This expression simplifies to

$$T_{AS} = \frac{1}{\beta + \gamma_A} + \frac{\beta}{\beta + \gamma_A} \frac{1}{\gamma_S + \delta} = T_A + p_{A \to S} T_S, \tag{27}$$

which is the average duration of being asymptomatic plus the average duration of being symptomatic times the probability of becoming symptomatic.

The infection fatality rate (IFR), that is, the probability of dying when symptomatic is

$$p_{S \to D} = \int_0^\infty \left(\delta e^{-\delta \tau} \right) e^{-\gamma_S \tau} d\tau = \frac{\delta}{\delta + \gamma_S}.$$

The probability of dying, conditional on being infected, is equal to the probability of making the transition from asymptomatic to symptomatic times the probability of dying when symptomatic

$$p_{E \to D} = p_{A \to S} p_{S \to D} = \frac{\delta}{\delta + \gamma_S} \frac{\beta}{\beta + \gamma_A}. \tag{28}$$

A.2 Reproduction rate with quarantine and contact tracing

A symptomatic individual who is not quarantined infects on average $\mathcal{R}_S = \alpha \left(S/N \right) R_S$ individuals until he recovers or dies, with

$$R_S = \int_0^\infty \tau \left[\left(e^{-\gamma_s \tau} \right) \left(\delta e^{-\delta \tau} \right) + \left(\gamma_S e^{-\gamma_s \tau} \right) \left(e^{-\delta \tau} \right) \right] d\tau = \frac{1}{\gamma_S + \delta}.$$

An asymptomatic individual who is not quarantined infects on average $\mathcal{R}_A = \alpha \left(S/N \right) R_A$ until she recovers or becomes symptomatic, with

$$R_A = \int_0^\infty \sigma \tau \left[\left(e^{-\gamma_A \tau} \right) \left(\beta e^{-\beta \tau} \right) + \left(\gamma_A e^{-\gamma_A \tau} \right) \left(e^{-\beta \tau} \right) \right] d\tau = \sigma \frac{1}{\gamma_A + \beta}.$$

An asymptomatic individual who is quarantined with rates ε_{QA} and ε_{QS} infects on average $\mathcal{R}_{AS} = \alpha \left(S/N \right) R_{AS}$ until he recovers or becomes symptomatic, with

$$R_{AS} \left(\varepsilon_{QA}, \varepsilon_{QS} \right) = \left(1 - \varepsilon_{QA} \right) R_A + \left(1 - \varepsilon_{QS} \right) \frac{\beta}{\gamma_A + \beta} R_S.$$

Let $\bar{R}_{AS}\left(\varepsilon_T, \varepsilon_{QA}, \varepsilon_{QS}\right)$ denote the expected infection factor for a latent individual (the individual of interest) before knowing whether the individual will be traced

$$\bar{R}_{AS}\left(\varepsilon_T, \varepsilon_{QA}, \varepsilon_{QS}\right) = \varepsilon_T R_{AS}\left(\varepsilon_{QA}, \varepsilon_{QS}\right) + \left(1 - \varepsilon_T\right) R_{AS}\left(0, \varepsilon_{QS}\right).$$

Consider an individual who is latent, traced with efficiency ε_T, and quarantined with rates ε_{QA} and ε_{QS}. The individual of interest may have been infected by (1) a symptomatic individual that was not quarantined, there are $(1 - \varepsilon_{QS}) I_S$ of them; (2) an asymptomatic individual that was traced, but not quarantined, there are $(1 - \varepsilon_{QA}) I_{AT}$ of them; and (3) an asymptomatic individual that was not yet traced, there are I_A of them. We want to calculate the average of new infections coming from this individual until she recovers or dies.

- Case 1 and 2: Since infectious individuals are only traced at the time they become symptomatic, the individual of interest will never be traced. Therefore, the expected number of new infections coming from the infected individual is
  $\mathcal{R}_{AS}\left(0, \varepsilon_{QS}\right) = \alpha\left(S/N\right) R_{AS}\left(0, \varepsilon_{QS}\right);$

- Case 3: The expected number of new infections coming from the infected individual when the infecting individual was asymptomatic is $\mathcal{R}_E = \alpha\left(S/N\right) R_E$, with $R_E =$

$$
\begin{aligned}
& \int_0^\infty \left[\gamma_A e^{-(\gamma_A+\beta)\tau_0}\right]\left[R_{AS}\left(0, \varepsilon_{QS}\right)\right] d\tau_0 \\
& + \int_0^\infty \left[\beta e^{-(\gamma_A+\beta)\tau_0}\right]\left[e^{-\phi\tau_0}\right]\bar{R}_{AS}\left(\varepsilon_T, \varepsilon_{QA}, \varepsilon_{QS}\right) d\tau_0 \\
& + \int_0^\infty \left[\beta e^{-(\gamma_A+\beta)\tau_0}\right]\left\{\int_0^{\tau_0}\left[\phi e^{-\phi s}\right]\left[e^{-(\gamma_A+\beta)(\tau_0-s)}\right]\left[\sigma\left(\tau_0 - s\right) + \bar{R}_{AS}\left(\varepsilon_T, \varepsilon_{QA}, \varepsilon_{QS}\right)\right] ds\right\} d\tau_0 \\
& + \int_0^\infty \left[\beta e^{-(\gamma_A+\beta)\tau_0}\right]\left\{\int_0^{\tau_0}\left[\phi e^{-\phi s}\right]\left[\int_0^{\tau_0-s}\left[\gamma_A e^{-(\gamma_A+\beta)t}\right]\left[\sigma t\right] dt\right] ds\right\} d\tau_0 \\
& + \int_0^\infty \left[\beta e^{-(\gamma_A+\beta)\tau_0}\right]\left\{\int_0^{\tau_0}\left[\phi e^{-\phi s}\right]\left[\int_0^{\tau_0-s}\left[\beta e^{-(\gamma_A+\beta)t}\right]\left[\sigma t + (1 - \varepsilon_{QS}) R_S\right] dt\right] ds\right\},
\end{aligned}
$$

where the five components of case 3 are

- Case 3.1: The infecting individual recovers at τ_0, and the infected individual is not traced;

- Case 3.2 through 3.5: The infecting individual becomes symptomatic at τ_0, and

  - Case 3.2: The infected individual never became asymptomatic;

  - Case 3.3: The infected individual became asymptomatic at s and stayed so until τ_0;

– Case 3.4: The infected individual became asymptomatic at s and recovered at $s + t$;

– Case 3.5: The infected individual became asymptomatic at s and symptomatic at $s + t$.

The probabilities for the components of case 3 are

$$p_{E1} = \frac{\gamma_A}{\gamma_A + \beta},$$

$$p_{E2} = \frac{\beta}{\gamma_A + \beta + \phi},$$

$$p_{E3} = \frac{\beta\phi}{2(\gamma_A + \beta + \phi)(\gamma_A + \beta)},$$

$$p_{E4} = \frac{1}{2}\frac{\beta\phi\gamma_A}{(\gamma_A + \beta)^2} \cdot \frac{1}{\gamma_A + \beta + \phi},$$

$$p_{E5} = \frac{1}{2}\frac{\phi\beta^2}{(\gamma_A + \beta)^2} \cdot \frac{1}{(\gamma_A + \beta + \phi)}.$$

The expected infections for the components of case 3 are

$$R_{E1} = \frac{\gamma_A}{\gamma_A + \beta}R_{AS}(0, \varepsilon_{QS}),$$

$$R_{E2} = \frac{\beta}{\gamma_A + \beta + \phi}\bar{R}_{AS}(\varepsilon_T, \varepsilon_{QA}, \varepsilon_{QS}),$$

$$R_{E3} = p_{E3}\left[\frac{\sigma}{2(\gamma_A + \beta)} + \bar{R}_{AS}(\varepsilon_T, \varepsilon_{QA}, \varepsilon_{QS})\right],$$

$$R_{E4} = \frac{\beta\phi\gamma_A\sigma}{4(\gamma_A + \beta + \phi)(\gamma_A + \beta)^3},$$

$$R_{E5} = \frac{\beta}{\gamma_A}[R_{E4} + p_{E4}(1 - \varepsilon_{QS})R_S],$$

and

$$R_E = \sum_{i=1}^{5} R_{E,i}.$$

A newly infected individual then infects on average $\mathcal{R} = \alpha(S/N)R$ individuals where

$$R = \frac{[(1 - \varepsilon_{QA})I_{AT} + (1 - \varepsilon_{QS})I_S]R_{AS}(0, \varepsilon_{QS}) + I_A R_E}{(1 - \varepsilon_{QA})I_{AT} + (1 - \varepsilon_{QS})I_S + I_A}.$$

A.3 Traceable individuals

We consider an asymptomatic infectious individual who is quarantined once he becomes symptomatic. For this case, we calculate the average number of exposed and infectious asymptomatic individuals that this individual has created.

By the time an asymptomatic individual becomes symptomatic, on average that individual has infected $\alpha(t) S(t)/N(t) R_{AT}$ other individuals, where

$$R_{AT} = \int_0^\infty (\sigma\tau) \left(\beta e^{-\beta\tau}\right) \left(e^{-\gamma_A\tau}\right) d\tau = \sigma \frac{\beta}{(\beta + \gamma_A)^2}.$$

The average number of individuals that the infectious individual has infected and that are not yet infectious at the time the individual becomes symptomatic is $\alpha(t) S(t)/N(t) R_{ATE}$, where

$$R_{ATE} = \int_0^\infty \sigma p_{EE}(\tau) \left[\beta e^{-(\beta + \gamma_A)\tau}\right] d\tau,$$

and the term in brackets is the probability that the infectious individual has been asymptomatic for duration τ, and $p_{EE}(\tau)$ denotes the fraction of individuals that were infected by the infectious individual over the interval τ and that have not yet become infectious at the time the individual becomes symptomatic. The probability that an individual that was infected time s ago and has not yet become infectious is $e^{-\phi s}$. Thus

$$p_{EE}(\tau) = \int_0^\tau e^{-\phi s} ds = \frac{1}{\phi}\left(1 - e^{-\phi\tau}\right)$$

and

$$R_{ATE} = \sigma \frac{\beta}{(\beta + \gamma_A)(\beta + \gamma_A + \phi)}. \tag{19}$$

The average number of individuals who an infectious individual has infected and that are infectious but asymptomatic at the time the individual becomes symptomatic is $\alpha(t) S(t)/N(t) R_{ATA}$, where

$$R_{ATA} = \int_0^\infty \left[\sigma \int_0^\tau p_{EA}(s) ds\right] \left[\beta e^{-(\beta + \gamma_A)\tau}\right] d\tau$$

and $p_{EA}(s)$ denotes the fraction of individuals that were infected time s ago, have become infectious in the meantime but have not yet recovered or become symptomatic. Thus

$$p_{EA}(s) = \int_0^s \phi e^{-\phi v} e^{-(\gamma_A + \beta)(s-v)} dv = \frac{\phi}{\phi - \gamma_A - \beta}\left[1 - e^{-(\phi - \gamma_A - \beta)s}\right]$$

and

$$R_{ATA} = \sigma \frac{\phi\beta}{2(\beta + \gamma_A)^2 (\beta + \gamma_A + \phi)}. \tag{20}$$

The average number of individuals that the infectious individual has infected and that have become symptomatic or recovered at the time the individual becomes symptomatic is $\alpha(t) S(t)/N(t) R_{ATR}$, where

$$R_{ATR} = \int_0^\infty \sigma \int_0^\tau p_{ER}(s) d\tau \left[\beta e^{-(\beta + \gamma_A)\tau}\right] d\tau$$

and $p_{ER}(s)$ denotes the fraction of individuals that were infected time s ago and that have recovered or become symptomatic,

$$p_{ER}(s) = \int_0^s \phi e^{-\phi v} \left[1 - e^{-(\gamma_A + \beta)(s-v)}\right] dv$$

and

$$R_{ATR} = \frac{\sigma \beta \phi}{2(\beta + \gamma_A)^2 (\beta + \gamma_A + \phi)} = R_{ATA}.$$

A.4 Robustness

In section 5.3.2, we have shown that the effectiveness of contact tracing turns out to be limited even though the environment is consistent with a large share of asymptomatic infected individuals. The environment was calibrated to match what is known about the spread of COVID-19, but the uncertainty about how the disease spreads is large. We now consider some alternative selections of parameter values and how they affect the effectiveness of contact tracing. One would expect that contact tracing becomes relatively more effective if there are relatively more asymptomatic infectious individuals or if asymptomatic individuals become relatively more infectious. The following two experiments suggest that neither of the two alternative calibrations increase the efficiency of contact tracing.

Table A1 reports results from alternative calibrations that increase the probability that asymptomatic infectious recover before they show symptoms. The top panel replicates the information from Table 2, columns 1 through 5, with baseline calibration $p_{A \to R} = 0.4$. The next two panels increase the recovery probability to 60 and 80 percent. For each of the two alternative calibrations we re-estimate the implied transmission rate. As we can see from comparing the upper left-hand side cells of each panel, $\varepsilon_Q = 0.5$ and $\varepsilon_T = 0.0$, the alternative employment path yields only slightly different cumulative deaths at the end of year for the different calibrations. Notice that without contact tracing, increasing quarantine efficiency has less of an impact when the share of asymptomatic infectious is larger, moving down column 1 of each panel in Table A1. Also, for any given quarantine efficiency, increasing contact tracing efficiency has a smaller impact on end-of-year cumulative deaths as the recovery probability increases. Essentially, once an infectious individual becomes symptomatic, fewer of the individuals who he infected are still around to be traced if asymptomatic individuals are recovering faster.

Table A2 reports results for alternative calibrations that increase the relative infectiousness of asymptomatic individuals. The top panel replicates the information from Table 2, columns 1 through 5, with baseline calibration $\sigma = 0.6$. The next two panels increase the relative infectiousness to 80 and 100 percent. We again re-estimate the implied transmission rate for each of the two alternative calibrations. Again, the alternative employment

Table A1: Share of Asymptomatic

ε_Q	(1)	(2)	(3)	(4)	(5)
			ε_T		
	0.000	0.250	0.500	0.750	1.000
			$p_{A\to R}$=0.40		
0.500	0.187	0.181	0.176	0.171	0.166
0.600	0.101	0.097	0.094	0.090	0.087
0.700	0.063	0.060	0.058	0.057	0.055
0.800	0.044	0.043	0.041	0.040	0.039
0.900	0.033	0.032	0.031	0.030	0.029
1.000	0.026	0.025	0.024	0.024	0.023
			$p_{A\to R}$=0.60		
0.500	0.190	0.187	0.184	0.182	0.179
0.600	0.107	0.106	0.104	0.102	0.101
0.700	0.069	0.068	0.067	0.066	0.065
0.800	0.050	0.050	0.049	0.048	0.048
0.900	0.039	0.039	0.038	0.038	0.037
1.000	0.032	0.031	0.031	0.030	0.030
			$p_{A\to R}$=0.80		
0.500	0.189	0.189	0.188	0.188	0.187
0.600	0.125	0.125	0.124	0.124	0.123
0.700	0.088	0.088	0.088	0.087	0.087
0.800	0.068	0.068	0.068	0.068	0.067
0.900	0.056	0.056	0.056	0.056	0.055
1.000	0.048	0.048	0.047	0.047	0.047

Note: Cumulative deaths at end of sample, December 31, 2020, as a percent of population for given recovery probability of asymptomatic individuals, $p_{A\to R}$, its implied alternative transmission path, and variations of quarantine efficiency, ε_Q, and tracing efficiency, ε_T, and no testing, $f = 0$. See also Table 2.

Table A2: Infectiousness of Asymptomatic

ε_Q	(1)	(2)	(3)	(4)	(5)
			ε_T		
	0.000	0.250	0.500	0.750	1.000
			$\sigma=0.60$		
0.500	0.187	0.181	0.176	0.171	0.166
0.600	0.101	0.097	0.094	0.090	0.087
0.700	0.063	0.060	0.058	0.057	0.055
0.800	0.044	0.043	0.041	0.040	0.039
0.900	0.033	0.032	0.031	0.030	0.029
1.000	0.026	0.025	0.024	0.024	0.023
			$\sigma=0.80$		
0.500	0.188	0.180	0.173	0.166	0.159
0.600	0.109	0.103	0.098	0.094	0.090
0.700	0.070	0.067	0.064	0.061	0.059
0.800	0.050	0.048	0.046	0.044	0.042
0.900	0.039	0.037	0.035	0.034	0.033
1.000	0.031	0.029	0.028	0.027	0.026
			$\sigma=1.00$		
0.500	0.188	0.178	0.170	0.162	0.154
0.600	0.115	0.108	0.102	0.096	0.091
0.700	0.076	0.072	0.068	0.064	0.061
0.800	0.056	0.053	0.050	0.047	0.045
0.900	0.043	0.041	0.039	0.037	0.035
1.000	0.035	0.033	0.031	0.030	0.028

Note: Cumulative deaths at end of sample, December 31, 2020, as a percent of population for given relative infectiousness of asymptomatic individuals, σ, its implied alternative transmission path, and variations of quarantine efficiency, ε_Q, and tracing efficiency, ε_T, and no testing, $f = 0$. See also Table 2.

path yields slightly different end-of-year cumulative deaths for each calibration. Notice that without contact tracing, increasing quarantine efficiency has less of an impact when the asymptomatic are more infectious since asymptomatic individuals are not quarantined and are relatively more infectious, moving down column 1 of each panel in Table A2. On the other hand, for any given quarantine efficiency, increasing contact tracing efficiency now has a larger impact on end-of-year cumulative deaths as the relative infectiousness increases.